# Accepted Manuscript


Influence of conductive nano- and microfiller distribution on electrical conductivity and EMI shielding properties of polymer/carbon composites

Yevgen Mamunya, Lyudmila Matzui, Lyudmila Vovchenko, Oleksii Maruzhenko, Viktor Oliynyk, Sławomira Pusz, Bogumiła Kumanek, Urszula Szeluga

PII: S0266-3538(18)31450-7

DOI: https://doi.org/10.1016/j.compscitech.2018.11.037

Reference: CSTE 7480

To appear in: *Composites Science and Technology*

Received Date: 18 June 2018

Revised Date: 19 October 2018

Accepted Date: 22 November 2018

Please cite this article as: Mamunya Y, Matzui L, Vovchenko L, Maruzhenko O, Oliynyk V, Pusz Sł, Kumanek Bogumił, Szeluga U, Influence of conductive nano- and microfiller distribution on electrical conductivity and EMI shielding properties of polymer/carbon composites, *Composites Science and Technology* (2018), doi: https://doi.org/10.1016/j.compscitech.2018.11.037.

# Influence of conductive nano- and microfiller distribution on electrical conductivity and EMI shielding properties of polymer/carbon composites

Yevgen Mamunya[1], Lyudmila Matzui[2], Lyudmila Vovchenko[2], Oleksii Maruzhenko[1], Viktor Oliynyk[2], Sławomira Pusz[3], Bogumiła Kumanek[3], Urszula Szeluga[3*]

[1]*Institute of Macromolecular Chemistry, National Academy of Sciences of Ukraine 48 Kharkivske chaussee, 02160 Kyiv, Ukraine*
[2]*Department of Physics, Taras Shevchenko National University of Kyiv, Volodymyrska str., 64/13, Kyiv, 01601, Ukraine*
[3]*Centre of Polymer and Carbon Materials, Polish Academy of Sciences, 34 Curie-Sklodowskiej, 41-819 Zabrze, Poland*

* Corresponding author: E-mail: uszeluga@cmpw-pan.edu.pl, Tel: +48 32 271 60 77.

**Abstract:** In this work, DC conductivity and EMI shielding characteristics in the frequency range of 25.5−37.5 GHz ($K_a$-band) of polymer composites based on ultrahigh-molecular-weight polyethylene (PE) and polypropylene (PP) containing different types of nano- and microfillers were studied. Graphene nanoplatelets (Gr), thermally exfoliated graphite (TEG), thermally treated anthracite (A) and dispersed metals such as iron (Fe) and copper (Cu) were used as conductive fillers. Two types of composites were formed: 1 – with ordered distribution of the filler particles in the form of conductive 3D network in polymer matrix (segregated structure), 2 – with random distribution of the filler particles. It was found that the percolation threshold for Gr and A filler is 100 and 10 times lower in the segregated system was 100 and 10 times lower than that for A filler with its random distribution in polymer matrix. Distinctly increased value of shielding efficiency ($SE_T$) in the segregated system can be explained by multiple internal reflection of electromagnetic wave in the network formed in the segregated structure. It was also found that the value of SE corresponds with the electrical conductivity of composites. However, for the same conductivity, higher values of SE were observed for the formed segregated structure in comparison with the literature data for composites with random filler distribution.

**Keywords:** A. Polymer-matrix composites (PMCs); A. Particulate-reinforced composites; A. Layered structures; Carbon fillers segregated structures; B. Electrical properties

## 1. INTRODUCTION

The widespread use of electronic and microelectronic devices brings the problem of generation, propagation and influence of radiation (EMR) energy on electronic equipment and the human

body. It causes the necessity for effective electromagnetic interference (EMI) shielding materials [1,2]. During the last two decades, the efforts of researchers have been focused on the design of shielding materials, which mainly have absorbing characteristics [3]. Conductive polymer composites (CPCs) are promising materials to be used as EMI shields because they offer light weight, low cost, good processability, and high resistance to corrosion [4,5]. The CPC shielding properties are realized via three mechanisms: reflection, absorption, and multiple reflections of electromagnetic radiation. Multiple reflections exist in polymer multicomponent composites where an EM wave reflects on the interfaces between the composite components. Many researchers focused on the EMI shielding materials used different carbon nanofillers: carbon black [6], graphite [7], carbon nanotubes (CNTs) [8-10], graphene materials [11,12], and mixed fillers: CNTs/glass fibers [13], graphene/carbon fibers [14], metal-coated carbon fibers [15], and graphite flakes/CNTs [16].

Segregated polymer composites (SPCs) can be a good solution for obtaining high shielding properties at low filler content. In SPCs, the conductive filler forms an ordered framework within a polymer, where conductive filler particles are located on boundaries between polymer grains. For segregated systems, the filler phase may be characterized by two concentration values: an average $\varphi$ calculated for the whole composite volume, and a local $\varphi_{loc}$ reflecting the real filler content in place of localization [17]. Evidently, the local concentration of the filler in the wall of the SPC framework is much higher than the mean filler concentration, $\varphi_{loc} >> \varphi$. The properties of composites, which can be related to the distance between particles and existence of contacts between them, such as electrical and thermal conductivity, dielectric and mechanical characteristics, are mostly defined by the local concentration of filler particles and shifted to lower values if the average concentration of filler is used [18]. Owing to this, the percolation threshold ($\varphi_c$) in a segregated system, defining the insulator/conductor transition, is much lower than that for composites with a random distribution of filler. Since the filler particles are packed closely in the wall of the framework at the filler content above (or well above) the percolation threshold, the

conductivity is essentially high at low filler content. Such a structure provides multiple reflections within a SPCs that increase the total absorption loss. Thus, SPCs promise essential advantages in shielding effect compared to CPCs having a random distribution of conductive filler. The most widely used way to process SPCs is a hot compacting method [19]. In the first stage, the mechanical mixture of polymer grains and filler powder with particle size *D* and *d*, respectively, is formed at a condition of $D>>d$. The fine filler particles cover the surface of bigger polymer particles, creating a "shell structure." After hot compacting (compression at the polymer softening temperature), the initial distribution of filler particles remains essentially unchanged on the boundaries between polymer grains and forms a segregated structure pattern, while the polymer particles are deformed and conglomerated under pressure, creating a solid polymer matrix. Processing conditions (temperature, compression time, mechanical and rheological properties of the polymer matrix), which influence the segregated structure, are very important for achieving decent electrical parameters of SPCs [19]. Lower temperature, short compression time and high viscosity of the polymer melt minimize the migration of filler particles into polymer grains, which reduces the $\varphi_c$ value. The ultrahigh molecular weight polyethylene (UHMWPE) is a preferred polymer material for the segregated composite [20]. Thus, UHMWPE was combined with CNTs [21,22], graphene [23] and graphene oxide [24] to prepare EMI shielding composites; e.g. the shielding effectiveness were equal to 70 dB at 70 mass% of Gr [23], 50 dB at 10 mass% of CNTs [21], and 33 dB at 0.66 vol.% of graphene oxide [24]. The use of SPCs as EMI shielding materials demonstrates a high level of EM absorption at small and moderate carbon filler contents, also with other polymers and fillers [25-29]. PP show similar usefulness for obtaining SPCs. This work is focused on the study of microstructure, electrical percolation behavior and shielding properties of PE-based SPCs as a function of the type and content of carbon filler particles. A comparative analysis of various SPCs and PP composites with a random distribution of the filler and an analysis of the shielding mechanism of the SPCs were conducted.

## 2. EXPERIMENTAL

### *2.1. Materials*

Three different types of carbon fillers were used to produce conductive composites, *i.e.*, nanofillers - graphene nanoplatelets (Gr), thermally exfoliated graphite (TEG) and microfiller - thermally treated anthracite (A). As a graphene filler, commercial graphene nanoplatelets N002-PDR with a true density ≤ 2.2 g/cm$^3$ , carbon content ≤ 97% and a specific surface area 400-800 m$^2$/g was used. The SEM micrograph of graphene nanoplatelets is shown in Fig. 1a. High-porosity powder of thermally exfoliated graphite has a highly developed active surface consisted of cellular structured particles with cell parameters given in Table 1 [30]. The image of TEG is presented in Fig. 1b.

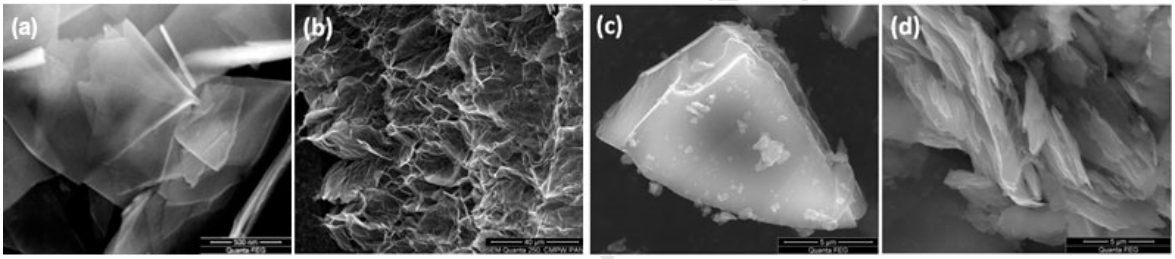


**Fig. 1.** SEM of the structures of Gr (a), TEG (b) and anthracite: raw (c) and thermally treated (d).

Table 1. Characteristics of polymers and fillers.

| Material | Density, g/cm$^3$ | Size of particles | Melting temperature, $^0$C |
|---|---|---|---|
| | Polymers | | |
| UHMWPE | 0.930 | 125/90 µm | 132 |
| PP | 0.905 | - | 165 |
| | Fillers | | Shape of particles |
| Anthracite (A) | 1.80 | 5 µm | irregular |
| Graphene (Gr) | <2.2 | XY - <10 µm, Z - <3 layers | lamellar |
| Thermoexfoliated graphite (TEG) | 1.85<br>0.005 (bulk density) | cells 5-10 µm, walls 40-80 nm | cellular |
| Copper (Cu) | 8.8 | 50 µm | dendritic |
| Iron (Fe) | 7.6 | 3 µm | spherical |

Recently, the bituminous coals (including anthracite) were proposed as fillers in polymer composites for various applications [31-34]. In this research the anthracite filler produced from

Svierdlovski (SV) anthracite is proposed as an alternative to graphene or graphite fillers. To produce anthracite fillers of better ordered graphite-like structure, the SV raw anthracite was thermally treated up to 2000 °C in $N_2$ atmosphere, and finally the carbon flake-shaped material was obtained. Detailed descriptions of this anthracite filler, *i.e.* its structure, characteristics and possible modification, were presented by Pusz et al. [31, 32]. The structures of SV anthracite, initial and after thermal treatment, are shown in Figs 1c and d. For experiments with EMI shielding the iron (Fe) and the copper (Cu) fillers with sizes and shape of particles given in Table 1 were also used.

UHMWPE Hostalen GUR (PE), type GHR 8110, supplied by Hoechst AG (Schkopau, Germany) in a powdered form with particle size 125/90 µm after sieving was used as the polymer matrix of segregated systems. Isotactic polypropylene PPH 7060 (PP) in a form of pellets was used to produce an anthracite/PP composite with a random distribution of filler particles. The characteristics of the polymers and fillers are given in Table 1.

### *2.2. Preparation of composites*

The hot compacting method was used to prepare samples of SPCs [18]. The mechanical mixture of PE and filler powder was homogenized by thoroughly triturating in a porcelain mortar to create the shell layer of carbon or metallic filler on the surface of the polymer particles. The mixture was then placed into a hot steel mold heated to 160 ºC and pressed (hot compacted) for 5 min at 50 MPa with subsequent cooling down of the mold to room temperature. Fig. 2 demonstrates the process of forming the segregated structure in a composite and a schematic diagram of segregated composite with different filler contents. The samples used for electrical measurements were produced in the form of discs with 30 mm diameter and 1÷2 mm height. For measurement of shielding parameters, samples 7.2 mm x 3.4 mm were cut from the discs.

Composites with a random distribution of filler were produced by an extrusion method using a laboratory one-screw extruder with screw ratio $l/d$=20. The temperature of the head-mold was 200 ºC. After extrusion, the strand was cut into small pieces and pressed at 180 ºC in the die described above.

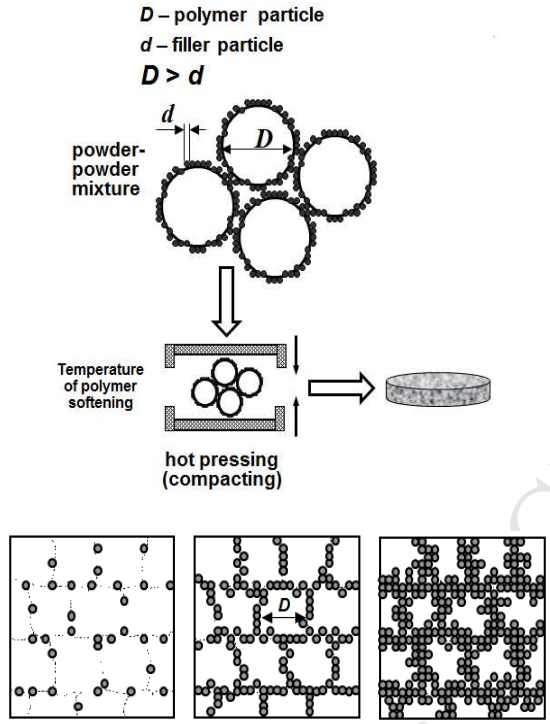


Fig. 2. The diagram of procedure of sample formation with segregated structure and the diagram of segregated systems with different amount of filler: below the percolation threshold, at the percolation threshold and above the percolation threshold (from left to right respectively).

### *2.3. Experimental methods*

The structures of carbon fillers were examined using the high-resolution scanning electron microscope FEI Quanta 250 FEG. Microscopic studies of composite samples were conducted with the reflected light optical microscope NJ120A (Ulab, China). The DC electrical conductivity $\sigma$ was measured using a two-contact scheme. A sample was held between two steel electrodes and measured under 100 V voltage using the E6-13 teraohmmeter Radiotechnika (Riga, Latvia). The values of $\sigma$ were estimated using the following Eq.:

$$\sigma = \frac{1}{R}\frac{h}{S} \qquad (1)$$

where $R$ is the experimentally measured electrical resistance, and $h$ and $S$ are the sample thickness and cross-sectional area, respectively.

Microwave measurements of electrodynamic characteristics of polymer composites were carried out using automated setups based on the network analyzer P2-65 (panoramic standing wave ratio (SWR) and attenuation meter) in the frequency range of 25.8–37.5 GHz. The principle of method is based on separate detections of the incident and reflected waves. To test the degree of interaction between microwaves and the polymer composites being studied, the specimens were fabricated as rectangular prisms and were placed in the waveguide cross-sections. Small signals proportional to the incident/reflected radiation power are tapped by the proper microwave directed couplers. The network analyzer performs the locked-in detection and the amplification of the incident wave signal $U_1$ and the reflected wave signal $U_2$. Both signals are used to calculate the reflection/attenuation coefficients and the results are converted via ADC to the accepted digital representation. Reflection index *R* and reflection loss *RL* (in dB) can be determined from measured standing wave ratio on voltage SWR and shielding effectiveness *SET* (in dB) is related to the measured EMR transmission index *T* using the following equations [35]:

$$R = \left( \frac{SWR - 1}{SWR + 1} \right)^2 \tag{2}$$

$$RL = 10 \log R \tag{3}$$

$$SE_T = 10 \log T \tag{4}$$

where $R = |E_R / E_I|^2$, $T = |E_T / E_I|^2$, $E_I$, $E_R$, $E_T$ are the electric field strengths of incident, reflected, and transmitted waves, respectively.

EMR absorption *A*, reflection *R* and transmission *T* indices are interrelated by equation of energy balance [35,36]:

$$A + T + R = 1 \tag{5}$$

The reflected and absorbed power are quantitative characteristics of power balance when electromagnetic radiation is incident on a shielding material, while EMR $SE_T$ is a relative quantity of the total EMR power, which may be presented as following [37,38]:

$$SE_T = SE_A + SE_R + SE_{MR}, \tag{6}$$

where $SE_A$ is the shielding factor due to the EMR absorption, $SE_R$ and $SE_{MR}$ are the shielding factors due to the reflection and multiple-reflection, respectively.

Authors [29] declare that $SE_{MR}$ can be neglected when $SE_T \geq 15$ dB. The EMI shielding efficiency towards reflection $SE_R$ and absorption $SE_A$ may be expressed as:

$$SE_R = 10\log(1-R), \qquad SE_A = 10\log\left(\frac{T}{1-R}\right). \tag{7}$$

Actually, $SE_A$ is a measure of the ability to attenuate the electromagnetic power that has transmitted into the shielding material.

## 3. RESULTS AND DISCUSSION

### *3.1. Electrical properties*

The segregated structure of PE filled with various contents of anthracite (A/PE) is shown in Fig. 3.

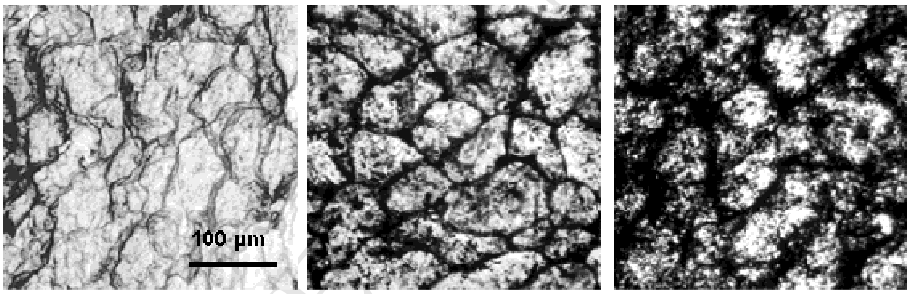


**Fig. 3.** The evolution of conductive phase formation with increasing anthracite filler content in segregated composite A/PE: a – 1 vol.%, below $\varphi_c$; b – 3 vol.%, at $\varphi_c$; c – 5 vol.%, above $\varphi_c$.

As observed, the filler particles are located at the interface between polymer grains and the thickness of the filler layer increases with filler content. When the filler concentration $\varphi$ reaches the percolation threshold ($\varphi_c$ = ~3 vol.%), the filler pattern becomes noticeable and provides the conductivity in the composite. Further growth of the filler amount leads to an increase in the framework wall thickness.

Fig. 4 shows the electrical conductivity of segregated systems with carbon fillers used, *i.e.*, Gr/PE, TEG/PE and A/PE, depending on the filler content. All the systems display the percolation behavior with very different values of percolation threshold. As shown, the percolation behavior is

characterized by essentially lower $\varphi_c$ values for composites containing Gr and TEG nanofillers in comparison to the anthracite microfiller. Clearly, smaller percolation thresholds $\varphi_c$=0.21 and 0.55 vol.% were observed for the composites Gr/PE and TEG/PE, respectively, probably owing to smaller sizes and better dispersity of Gr and TEG particles in the matrix in comparison to the anthracite filler. The inset in Fig. 4 demonstrates the percolation behavior in the A/PP composite, with a random distribution of the filler, and in the A/PE composite, where anthracite creates a segregated structure (it can be considered that the nature of the polymer does not essentially influence the electrical properties of the composite). $\varphi_c$ for the segregated composite is much lower (~3 vol.%) than that for the composite with random filler distribution (~25 vol.%). This demonstrates the importance of local filler concentration $\varphi_{loc}$ in the segregated structure, which is much higher than the average filler concentration $\varphi$, $\varphi_{loc}>>\varphi$, and defines the low value of the percolation threshold. At random filler distribution, the local and average concentrations are identical, $\varphi_{loc}=\varphi$, and the value of $\varphi_c$ is much higher.

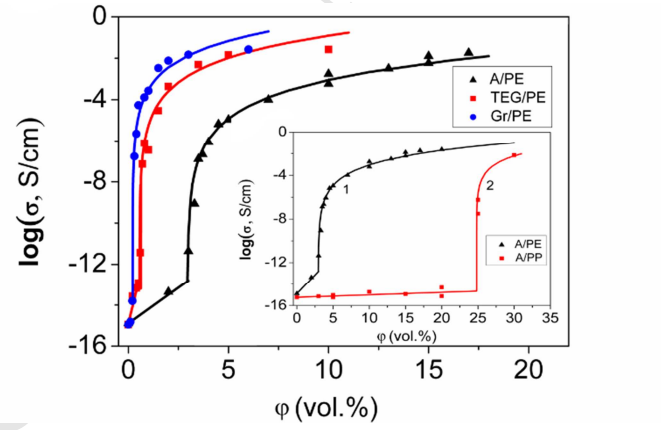


**Fig. 4**. Concentration dependence of conductivity for composites with segregated structure and different carbon fillers. Inset shows the concentration dependence of conductivity for composites with anthracite for: (1) segregated structure, (2) random distribution of A filler. Points are experimental values, lines correspond to the calculations from Eq. (8) for the region $\varphi > \varphi_c$.

The electrical conductivity behavior above the percolation threshold is described by the relation [39]:

$$\sigma = \sigma_0 (\varphi - \varphi_c)^t \qquad (8)$$

where $t$ is the critical exponent, and $\sigma_0$ is the adjustable parameter depending on filler conductivity. As it is seen from Fig. 4, the fitted curves (solid lines) obtained using the percolation model (Eq. 8) agree well with the experimental data. The values of the parameters of Eq. (8) are given in Table 2.

Table 2. Parameters of Eq.(8) for the composites studied.

| Composite | $\varphi_c$, vol.% | $t$ | $\sigma_0$, S/cm |
|---|---|---|---|
| A/PE | 2.95 | 3.5 | $9.6 \cdot 10^0$ |
| Gr/PE | 0.21 | 3.0 | $6.6 \cdot 10^2$ |
| TEG/PE | 0.55 | 3.3 | $3.0 \cdot 10^2$ |
| A/PP | 24.8 | 2.5 | $9.6 \cdot 10^0$ |

The critical exponent $t$ reflects the dimensionality of the system and the universality class of the problem. For a three-dimensional random percolation, $t$ is close to 2.0 [39]. For all segregated systems, the $t$ values re clearly higher than the theoretical value, while for the A/PP composite with random filler distribution, $t$=2.5, closer to that predicted by the theory. The reason for this effect may be the ordered, non-statistical distribution of filler particles. $\sigma_0$ depends on the conductivity of filler particles [40], and thus, according to the data from Table 2, the Gr has the highest conductivity among those used in this study.

### *3.2. EMI shielding properties*

#### *3.2.1.Reflection loss and shielding efficiency*

The high-performance electrical conductivity of the prepared segregated polymer composites would help to develop efficient EMI shielding materials, especially at ultralow conductive filler loading. The segregated structure forms a conducting framework in the composite, leading to increased conductivity and EMI shielding efficiency.

Shielding efficiency $SE_T$ and reflection loss $RL$ as a function of frequency for PE SPCs with various conductive particles are shown in Fig. 5.

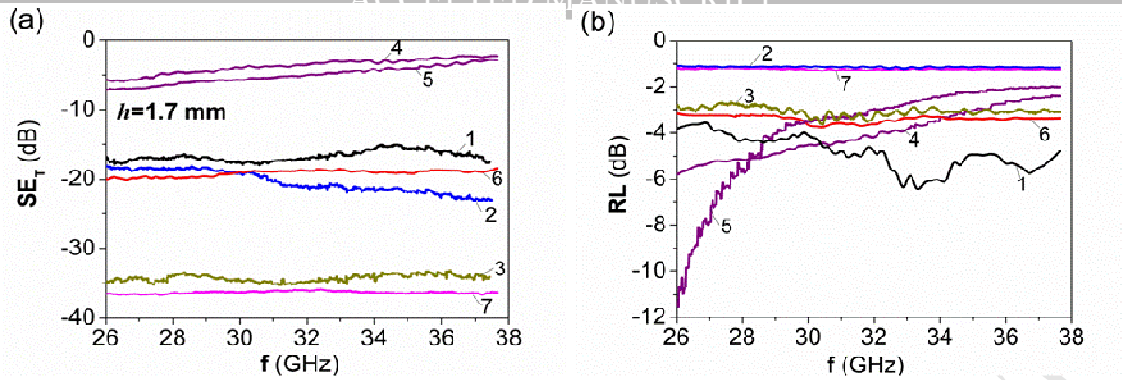


**Fig. 5.** Shielding efficiency $SE_T$ (a) and reflection loss $RL$ (b) for PE composites with metal and combined carbon/metal fillers in the frequency range 26-37.5 GHz: 1 - 20Fe/PE, 2 - 10Cu/PE, 3 - 20Cu/PE, 4 - 2.5A/2.5Fe/PE, 5 - 2.5A/2.5Cu/PE, 6 - 10A/10Fe/PE, 7 - 10A/10Cu/PE. Samples thickness 1.7 mm.

Table 3 summarizes the data on DC electrical conductivity, shielding efficiency $SE_T$ and parts of shielding efficiency consisting of reflection $SE_R$ and absorption $SE_A$ at 27 GHz (defined from the experimental data on power EMR reflection ($R$) and transmission ($T$) indexes using Eq.(7) ) for PE composites with Gr and TEG nanofillers, as well as with anthracite and metallic particles as microfillers.

**Table 3**. Shielding properties (at 27 GHz) of composites with metallic, combined metal/carbon and various carbon fillers (number before type of filler means its volume content in vol.%).

| Composition | $\sigma$ , S/cm | $SE_T$, (-dB) | $SE_R$, (-dB) | $SE_A$, (-dB) |
|---|---|---|---|---|
| | $h$=1.7mm | | | |
| 20Fe/PE | $3.7\cdot10^{-3}$ | 16.9 | 2.4 | 14.5 |
| 10Cu/PE | $4.1\cdot10^{-2}$ | 15.1 | 3.1 | 12.0 |
| 20Cu/PE | $2.3\cdot10^{-1}$ | 37.7 | 6.4 | 31.3 |
| 2.5A/2.5Fe/PE | $2.3\cdot10^{-7}$ | 5.6 | 1.5 | 4.1 |
| 2.5A/2.5Cu/PE | $1.1\cdot10^{-6}$ | 7.4 | 1.3 | 6.1 |
| 10A/10Fe/PE | $1.9\cdot10^{-3}$ | 18.8 | 2.8 | 16.0 |
| 10A/10Cu/PE | $7.9\cdot10^{-3}$ | 36.6 | 6.2 | 30.4 |
| | $h$=1mm | | | |
| 1TEG/PE | $8.5\cdot10^{-7}$ | 4.9 | 2.52 | 2.30 |
| 3.5TEG/PE | $7.1\cdot10^{-3}$ | 23.7 | 3.57 | 20.1 |
| 5TEG/PE | $2.6\cdot10^{-2}$ | 37.0 | 5.53 | 31.5 |
| 20A/PP (random) | $2.0\cdot10^{-15}$ | 7.2 | 4.32 | 2.9 |
| 20A/PE | $3.0\cdot10^{-2}$ | 33.0 | 5.69 | 27.3 |

| | | | | |
|---|---|---|---|---|
| 2Gr/PE | $1.0 \cdot 10^{-2}$ | 22.7 | 3.28 | 19.4 |

As seen in Fig. 5a and Table 3, the composite with 20 Cu (here and going further, the number in front of the type of the filler means its content in vol.%) has a high value of $|SE_T|$ = 37.7 dB due to high filler conductivity. However, substitution of half amount of metal by less conductive anthracite (hybrid composite with 10 A/10 Cu combined filler) does not sufficiently decrease the shielding efficiency, $|SE_T|$ = 36.6 dB. Despite the 30 times loss in total conductivity (see Table 3), this hybrid composite demonstrates high shielding effectiveness in comparison to the 20 Cu/PE composite. Similar behavior is observed for 20Fe/PE and 10A/10Fe/PE composites. This can be the effect of the higher dispersity of anthracite than copper filler and the presence of a stacked structure of carbon planes (layers) within the individual particle (see Fig. 1d), which increases multiple reflections of electromagnetic waves inside the anthracite particles. This indicates a promising way to use combined fillers to lighten the weight of shielding materials. Comparing the data on shielding terms $SE_R$, $SE_A$ and $SE_T$, it can be concluded that the maximal $SE_T$ is mainly related to the high absorption term $SE_A$ and explained by the high content (20 vol.%) of conductive particles - Cu or A/Cu, which effectively interact with electromagnetic waves. Composites with low anthracite/metal filler content (2.5 A/2.5 metal) have the lowest $|SE_T|$ (5÷7 dB), while composites with only metal fillers (20 Fe and 10 Cu) or with medium amounts of combined metal/anthracite fillers (10 A/10 Fe) have intermediate $|SE_T|$ values (15÷17 dB). The *RL* (Fig. 5b) and $SE_R$ (Table 3) show that more conductive composites possess higher reflection characteristics.

As seen from the data presented in Fig. 6 for composites with carbon fillers, a high shielding efficiency ($|SE_T|$ between 33-37 dB) is observed for composites with 20 vol.% of anthracite and 5 vol.% of TEG.

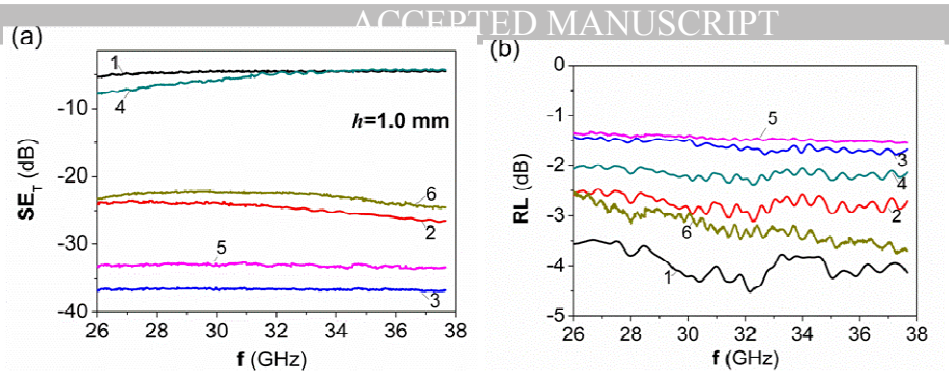


**Fig. 6.** Shielding efficiency $SE_T$ (a) and reflection loss $RL$ (b) for PE and PP based composites with various carbon fillers in the frequency range 26-37.5 GHz: 1 - 1TEG/PE, 2 - 3.5TEG/PE, 3 - 5TEG/PE, 4 - 20A/PP, 5 - 20 A/PE, 6 - 2Gr/PE. Thickness of samples $h$ =1.0 mm.

This result demonstrates sufficiently higher shielding effectiveness of TEG nanofiller in comparison to anthracite microfiller, despite the specific structure of anthracite filler, which showed its effectiveness in combination with metal (see Table 3). The least $|SE_T|$ values are obtained for the 20 A/PP composite with a random distribution of anthracite filler (7.2 dB) and for low-filled PE (segregated system) with 1 vol.% of TEG (4.9 dB). Both composites also have low conductivity, 20 A/PP because the filler concentration is below the percolation threshold and 1TEG/PE composite because the filler concentration is slightly higher than $\varphi_c$. However, segregated composites with 3.5 vol.% TEG and 2 vol.% Gr present similar intermediate values of $|SE_T|$, 23.7 dB and 22.7 dB, respectively (see Table 3).

An interesting combination of EMI parameters is demonstrated by the 20A/PP sample with a random distribution of filler particles. The absorption $SE_A$ parameter is very low since it is a nonconductive composite, while the reflectance $SE_R$ value is on the level of the most conductive composites. Thus, if the absorption process follows the presence of conductivity in a composite, for reflectance it is important to have the presence of a massive phase created by conductive particles (which do not form a conductive cluster). These isolated conductive particles can be considered as "artificial dipoles," which are polarized in an electric field and induce relatively large dielectric permittivity $\varepsilon_r'$ of such composites that, in turn, increase their reflective properties. In

addition, the electromagnetic wave interacts with the skin layer of every separated conductive particle that leads to total interference and reflectance on the composite surface.

### *3.2.2. Internal multiple reflections in segregated PE-based composites*

In segregated composites, the internal reflection effect might be not ignored in predicting shielding properties. Since the PE granules in composites are coated by conductive filler particles, there are many interphase areas for internal reflection of EMR on the conductive framework and, as a result, the increase of effective shielding due to absorption in the segregated structure occurs. It is possible to say that internal reflection in segregated systems, included in the $SE_A$ parameter, increases the absorption part of their shielding effectiveness.

At the first approximation, the segregated structure can be considered as a set of small multilayered blocks with alternating thick polymer and thin filler layers, as shown in Fig. 7. For the multilayered shields [34, 41, 42], such quasi-periodic arrangement of low and high conductivity materials occurring within the SPCs promotes the high absorption of EMR due to multiple internal reflections.

Fig. 7 demonstrates that incident power $P_{in}$ decreases running along the segregated structure and losing small parts of $P$ at reflection on every polymer-filler block.

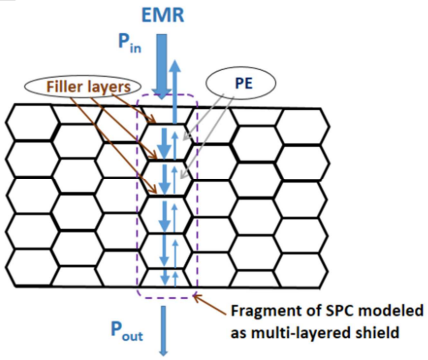


**Fig. 7.** Schematic representation of multiple reflection in the segregated composite structure.

As a result, the transmitted power $P_{out}$ is much lower because of multiple internal reflections, which plays a role in the absorbing part. As mentioned by authors [26,29], composites possessing shielding effectiveness ≥ 20 dB are fit for application in industrial fields as protective materials. All

segregated composites studied with filler contents 2Gr, 3.5TEG, 5TEG and 20A satisfy this condition, but in the case of Gr and TEG, such high efficiency is reached at small concentrations of the nanofillers. Anthracite, as a microfiller, requires a large content of particles in the composite to provide a high level of $SE_T$. Thus, the 20A/PE composite shows a comparable value of $|SE_T|$ (33 dB) with 5TEG/PE composite (37 dB). Hence, possible to conclude that nanofillers with high aspect ratios cover the PE grains with more entire layers and create more perfect and dense frameworks in the polymer.

### *3.2.3. The relation between EMI reflection, absorption properties and electrical conductivity of segregated PE-based composites*

Another interesting problem is the extent to which the conductivity of composites affects their shielding characteristics. EMI shielding efficiency $SE_T$ can be written as a function of the impedance of the material ($\eta$ and $\eta_0$), the thickness of sample *h*, and the skin depth $\delta$ [43,44]:

$$SE_T = SE_A + SE_R + SE_{MR} = 20\log\left(e^{\frac{h}{\delta}}\right) + 20\log\left(\frac{\eta}{4\eta_0}\right) + 20\log\left(1 - e^{\frac{2h}{\delta}}\right) \qquad (9)$$

The thickness of the skin layer indicates the depth at which the EMR is e times weakened and is a function of frequency *f*, magnetic permeability $\mu$ and conductivity $\sigma$:

$$\delta = (\pi f \mu \sigma)^{-0.5} \qquad (10)$$

Skin depth decreases with an increase in material conductivity, magnetic permeability and frequency of EM energy. Impedance $\eta = |E| / |H|$ can be written as follows [43, 44]:

$$\eta = \left(\frac{2\pi f \mu}{\sigma}\right)^{0.5}; \quad \eta_0 = \left(\frac{\mu_0}{\varepsilon_0}\right)^{0.5} \quad . \qquad (11)$$

Taking into account Eqs (9) - (11), the expressions of the absorption $SE_A$ and the reflection $SE_R$ effectiveness take the following forms [44-47]:

$$SE_A = C_1 + C_2 h (f \mu \sigma)^{0,5} \qquad (12)$$

$$SE_R = C_3 + 10 log\left(\frac{\sigma}{2\pi f \mu}\right) \qquad (13)$$

$$SE_T = SE_A + SE_R \quad (14)$$

where $C_1$ = 4 dB means absorption at low concentrations and low conductivity of the filler. The values of the coefficients $C_2$ and $C_3$ are equal to 0.0015 and 108, respectively, and coincide with the ones given in [46] and [47]. As was mentioned, the $SE_{MR}$ parameter can be neglected.

As follows from Eqs (12) and (13), both parameters, $SE_A$ and $SE_R$, grow with increasing conductivity $\sigma$. Thomassin et al. [48] specify that both absorption and reflection increase with increasing conductivity; however, the increase in $SE_A$ is more important than that in $SE_R$. A strategy based on increasing the conductivity and higher filler content is not an efficient way to reach high shielding efficiency. To obtain a higher proportion between $SE_A$ and $SE_R$, different ways of arranging the structure of the shield material should be applied. One of them is creating the segregated structure of conductive filler in a composite.

The relations between shielding effectiveness parameters ($SE_A, SE_R, SE_T$) and conductivity $\sigma$ for $f$ = 27 GHz for all composites studied were obtained using Eqs (12)-(14) and presented in Fig. 8. As seen in Fig. 8a, the experimental results coincide well with the calculated $SE_A$ curve for all composites, with the exception of Cu/PE. These data show that a noticeable increase in the absorption effectiveness $SE_A$ of this composite begins when its conductivity exceeds $\sigma = 10^{-3}$ S/cm. For the Cu/PE composite, such an increase in $SE_A$ is observed at a conductivity value an order of magnitude higher. The lower efficiency of this system may be explained by the large size (~50 μm) of Cu filler particles. The $SE_R$ calculation (Fig. 8b) shows a very sharp dependence on the increase in conductivity, while with conductivity values less than $10^{-2}$ S/cm, $SE_R$ passes into the negative region. Authors [44] note that in order to have positive values for $SE_R$, the conductivity must be higher than 1 S/m.

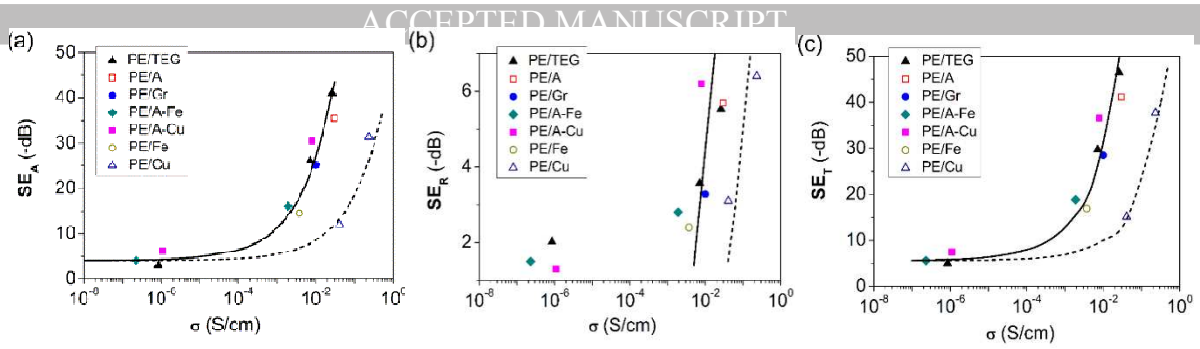


**Fig. 8.** Relationship between conductivity $\sigma$ and shielding effectiveness parameters of absorption $SE_A$, reflection $SE_R$ and total $SE_T$. Symbols are experimental values for different systems (corresponding to those given in Table 3 and reduced to a thickness of 1.7 mm data for carbon/PE composites), solid lines are calculations with Eq. (12) - (14) for carbon and hybrid fillers, dashed line is calculation for Cu/PE composite.

For the Cu/PE composite, such an increase in $SE_A$ is observed at a conductivity value an order of magnitude higher. The lower efficiency of this system may be explained by the large size (~50 μm) of Cu filler particles. that, in turn, leads to the small specific surface of the filler with large particles.

The $SE_R$ calculation (Fig. 8b) shows a very sharp dependence on the increase in conductivity, while with conductivity values less than $10^{-2}$ S/cm, $SE_R$ passes into the negative region. Authors [43] note that in order to have positive values for $SE_R$, the conductivity must be higher than 1 S/m. $SE_T$ calculated by Eq. (14) (Fig. 8c) are also well correlated with experimental data, revealing the same patterns as previous dependencies.

Fig. 9 shows the relationship between electrical conductivity $\sigma$ of composites and their $SE_T$ and $SE_R$, based on the literature data [9, 44, 46-55] for systems with random distributions of filler were studied. The increase in $SE_T$ for different composites is observed in the range of their conductivity values, which overlap by three decimal orders, from $10^{-3}$ to $10^{0}$ S/cm. In all systems studied, with the exception of [46], the fillers used were single-walled and multi-walled nanotubes, but the polymers were different. Apparently, the method of preparation of composites, type of nanotubes

and their distribution in the volume of polymer matrix exert a strong influence on the electrical and shielding characteristics of composites, which is a source of rather wide scattering.

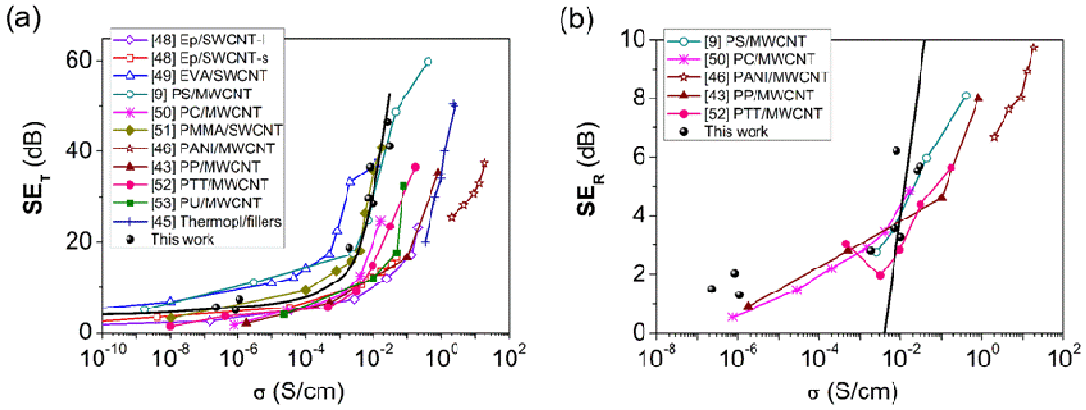


**Fig. 9.** a) - the relationship between conductivity and shielding effectiveness SE according to the literature data and the results of this study; b) - the effect of conductivity on reflection effectiveness $SE_R$. The symbols are experimental values, black solid lines are calculated by Eqs (12) - (14).

It can be seen in Fig. 9 that the increase of shielding effectiveness for composites obtained in this study occurs at lower conductivity values and, correspondingly, at lower filler concentrations, than was described in the cited references. The exception is the EVA-SWCNT composite [51], but its better shielding properties can be caused by the large thickness of the sample (3.5 mm), while the thickness of other composites was between 1-2 mm. The major reason for the good shielding effect at lower conductivity is the segregated structure of the composites, which, as shown above, is more effective for absorbing electromagnetic energy compared to systems containing randomly distributed filler particles. A comparison of SPCs and composites with a random filler distribution towards shielding effectiveness demonstrates the crucial role of the spatial arrangement of conductive filler particles in the volume of the polymer. Formation of a regular framework with a period equal to a size of polymer grains and consisting of conductive particles with high local concentration $\varphi_{loc}$ leads to a high efficiency of electromagnetic radiation absorption at a low average concentration of conductive filler in a composite. Nano-sized particles of carbon filler turned out to be more effective in creating an absorbing framework than carbon particles of larger micro-size. The experimental values of $SE_R$ obtained for the composites studied coincide with the

literature data (Fig. 9b). Meanwhile, the theoretical calculation of this parameter by Eq. (13) is poorly consistent with the experimental data and demonstrates a too-sharp dependence on conductivity in comparison with the experimental values of $SE_R$, which grow more smoothly.

### *3.2.4. Influence of a sample thickness on the shielding efficiency*

Since the $SE_A$ depends on the shield thickness (see Eq. (12)), the published data for the dependence of $SE_T$ on the thickness of samples are analyzed [28, 44, 51, 53, 55]. The results are shown in Fig. 10.

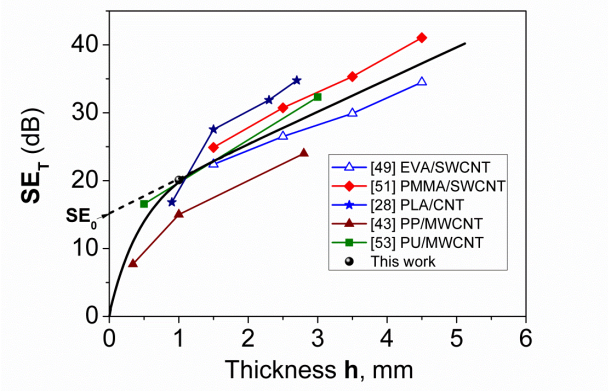


**Fig. 10**. Dependence of shielding effectiveness on the sample thickness. The line is guided by the eye.

The criterion of thickness of the shield in Eq. (9) is the $h/\delta$ ratio. The skin depth $\delta$ in the conductive composite can be estimated from the following equation [44]:

$$SE_A = 8.7\frac{h}{\delta} \qquad (15)$$

Assuming $h$ =1.5 mm and $SE_A$=15 dB, this estimation gives $\delta$ =0.87 mm. Consequently, such a decrease in the shield thickness, when the value of $h$ approaches the value of $\delta$ (the ratio reaches $h/\delta = 1$), leads to a decrease in the overall efficiency $SE_T$ due to the contribution of $SE_{MR}$. As Gonzales et al. [43] noted, a contribution of multiple reflections in shielding efficiency can be neglected when the sample is thicker than the skin. According to Zang et al. [55], the mechanism of total $SE_T$ changes when the ratio $h/\delta$ reaches 1.3.

$SE_0$ is the minimum shielding efficiency, above which the contribution of multiple reflections becomes negligible and the dependence of $SE_T$ on the shield thickness is determined only by the term $SE_A$ of Eq. (9). Indeed, the multiple reflections are negligibly small when $SE_T$ exceeds 15 dB [16, 29, 56].

**CONCLUSIONS**

Polymer composites based on UHMWPE and carbon nano- and microfillers create a segregated structure that consists of the ordered distribution of filler particles within a polymer matrix in the form of a regular framework with a period equal to the size of polymer grains. The segregated structure may be characterized by two values of filler concentration, $\varphi_{loc}$ being a true local filler concentration in the wall of the framework and $\varphi$, which is a mean concentration of a filler related to the entire volume of the polymer matrix, with the condition $\varphi_{loc} \gg \varphi$.

This fact results in a low percolation threshold with values between 0.21 – 2.95 vol.% for the segregated structure versus 24.8 vol.% for a random distribution of filler in composites filled with carbon nanofillers (Gr and TEG), and carbon microfiller (thermally treated anthracite).

The increase in electrical conductivity of composites along with increasing carbon filler content leads to an essential increase in $SE_A$ and $SE_T$. In segregated polymer composites, shielding parameters considerably increase due to absorption caused by internal reflection on conductive walls of the framework, consisting of a high concentration $\varphi_{loc}$ of conductive filler particles.

It was found that carbon nanofillers create the most effective framework, which provides a high level of EMR absorption at low concentration. For example, comparable $SE_T$ values are achieved for the nanofillers TEG (3-5 vol.%), Gr (2 vol.%) and for the microfillers A, Cu and Fe (20 vol.%). On the other hand, the anthracite microfiller showed prominent properties being combined with metal filler. A hybrid composite with combined A/Cu filler (10A/10Cu) revealed $SE_T$ comparable to that of 20 vol. % of Cu despite the lower conductivity of the

anthracite. The reason for this effect can be its specific structure consisting of stacked carbon planes that cause the phenomena of multiple reflections of electromagnetic waves.

Obtained results indicate a promising way to use carbon nanosized and microsized fillers as effective shielding materials in different areas of application.

A comparison of the conductivity effect on shielding effectiveness for composites with the segregated structure obtained in this work and the literature data for composites with random filler distribution shows the ability of the segregated structures to impart shielding properties to the composite with lower conductivity and, correspondingly, a lower concentration of conductive filler.

$SE_T$ decreases rapidly when the thickness of the shield sample approaches the skin depth due to the contribution of the negative term $SE_{MR}$. Above a sample thickness of 1.5 mm, the dependence $SE_T = f(h)$ is linear due to the contribution of $SE_A$, while the multiple reflection $SE_{MR}$ becomes negligible.

**Acknowledgement**

Ye. Mamunya and O. Maruzhenko acknowledge financial support of the project 31-H (2015-2019) of the Complex program of fundamental studies of the NAS of Ukraine “Fundamental problems of development of novel nanomaterials and nanotechnologies”. This work was partially realized in the frame of Polish-Ukrainian joint project "Development of newest polymer nanocomposites with high performance using the perspective carbon filler - anthracite as an analogue of graphene".

**References**

1. S.K. Dhawan, A. Ohlan, and K. Singh, Designing of nano composites of conducting polymers for EMI shielding, in: B. Reddy (Eds.), Advances in nanocomposites - synthesis, characterization and industrial applications, InTech., Croatia, 2011, pp. 429-482.
2. O. Yavuz, M.K. Ram, M. Aldissi, Electromagnetic applications of conducting and nanocomposite materials, in: V. Erokhin, M.K. Ram, O. Yavuz (Eds.), The new frontiers of organic and composite nanotechnology, Elsevier, Oxford, 2008, pp. 435-475.
3. H. Wang, D. Zhu, W. Zhou, F. Luo, Effect of multiwalled carbon nanotubes on the electromagnetic interference shielding properties of polyimide/carbonyl iron composites, Ind. Eng. Chem. Res. 54 (2015) 6589-6595.

4. A. Ameli, M. Nofar, S. Wang, and C.B. Park, Lightweight polypropylene/stainless-steel fiber composite foams with low percolation for efficient electromagnetic interference shielding, ACS Appl. Mater. Interfaces 6 (2014) 11091-11100.
5. S. Biswas, G.P. Kar, S. Bose, Tailor-made distribution of nanoparticles in blend structure toward outstanding electromagnetic interference shielding, ACS Appl. Mater. Interfaces 7 (2015) 25448-25463.
6. S.P. Mahapatra, V. Sridhar, and D. K. Tripathy, Impedance analysis and electromagnetic interference shielding effectiveness of conductive carbon black reinforced microcellular EPDM rubber vulcanizates, Polym. Compos. 29 (2008) 465-472.
7. V. Panwar, R.M. Mehra, J-O Park, and S.Park, Dielectric analysis of high-density polyethylene-graphite composites for capacitor and EMI shielding application, J. Appl. Pol. Sci. 125 (2012) E610–E619.
8. S. Bal, and S. Saha, Scheming of microwave shielding effectiveness for X band considering functionalized MWNTs/epoxy composites, Mater. Sci. Eng. 115 (2016) 012027-9.
9. M. Arjmand, T. Apperley, M. Okoniewski, and U. Sundararaj, Comparative study of electromagnetic interference shielding properties of injection molded versus compression molded multi-walled carbon nanotube/polystyrene composites, Carbon 50 (2012) 5126-5134.
10. J. Lin, H. Zhang, P. Li, X. Yin, Y. Chen, and G. Zeng, Electromagnetic shielding of multiwalled, bamboo-like carbon nanotube/methyl vinyl silicone composite prepared by liquid blending, Compos. Interfaces 21 (2014) 553-569.
11. AhA Al-Ghamdi, AtA Al-Ghamdi, Y. Al-Turki, F. Yakuphanoglu, and F. El-Tantawy, Electromagnetic shielding properties of graphene/acrylonitrile butadiene rubber nanocomposites for portable and flexible electronic devices, Composites Part B 88 (2016) 212-219.
12. D.-X. Yan, H. Pang, B. Li, R. Vajtai, L. Xu, P.-G. Ren, J.-H. Wang, and Z.-M. Li, Structured reduced graphene oxide/polymer composites for ultra-efficient electromagnetic interference shielding, Adv. Funct. Mater. 25 (2015) 559-566.
13. L.V. Silva, S.H. Pezzin, M.C. Rezende, S.C. Amico, Glass fiber/carbon nanotubes/epoxy three-component composites as radar absorbing materials, Polym. Compos. 37 (2016) 2277-2284.
14. V. Li, Y. Zhao, J. Sun, Y. Hao, J. Zhang, X. Han, Mechanical and electromagnetic interference shielding properties of carbon fiber/graphene nanosheets/epoxy composite, Polym. Compos. 37 (2016) 2494-2502.
15. X. Huang, B. Dai, Y. Ren, J. Xu, and P. Zhu, Preparation and study of electromagnetic interference shielding materials comprised of Ni-Co coated on web-like biocarbon nanofibers via electroless deposition, J. Nanomater. (2015) Article ID 320306:7 pages.
16. S. Maiti, N.K. Shrivastava, S. Suin, and B.B. Khatua, Polystyrene/-MWCNT/Graphite nanoplate nanocomposites: efficient electromagnetic interference shielding material through Graphite nanoplate−MWCNT−Graphite nanoplate networking, ACS Appl. Mater. Interfaces 5 (2013) 4712-4724.
17. Y.P. Mamunya, V.V. Davydenko, P. Pissis, and E.V. Lebedev, Electrical and thermal conductivity of polymers filled with metal powders, Eur. Polym. J. 38 (2002) 1887-1897.
18. Y. Mamunya, Carbon nanotubes as conductive filler in segregated polymer composites - electrical properties, in: S. Yellampalli (Eds.), Carbon nanotubes – polymer nanocomposites, InTech, Croatia, 2011, pp.173-196.

19. H. Pang, L. Xu, D.-X. Yan, and Z.M. Li, Conductive polymer composites with segregated structures, Prog. Polym. Sci. 39 (2014) 1908-1933.
20. C. Zhang, C.-A. Ma, P. Wang, and M. Sumita, Temperature dependence of electrical resistivity for carbon black filled ultra-high molecular weight polyethylene composites prepared by hot compaction, Carbon 43 (2005) 2544-2553.
21. M.H. Al-Saleh, Influence of conductive network structure on the EMI shielding and electrical percolation of carbon nanotube/polymer nanocomposites, Synth. Met. 205 (2015) 78-84.
22. H. Pang, Y. Bao, S.-G. Yang, C. Chen, W.-Q. Zhang, J. Chen, X. Ji, and J. Lei, Preparation and properties of carbon nanotube/binary-polymer composites with a double-segregated structure, J. Appl. Polym. Sci. (2014) doi: 10.1002/APP.39789.
23. M.H. Al-Saleh, Electrical and electromagnetic interference shielding characteristics of GNP/UHMWPE composites, J. Phys. D: Appl. Phys. 49 (2016) 195302-7.
24. D.-X. Yan, H. Pang, L. Xu, Yu. Bao, P.-G. Ren, J. Lei, and Z.-M. Li, Electromagnetic interference shielding of segregated polymer composite with an ultralow loading of in situ thermally reduced graphene oxide, Nanotechnology 25 (2014) 145705-5.
25. H. Wang, K. Zheng, X. Zhang, T. Duc, C. Xiao, X. Ding, C. Bao, L. Chen, and X. Tian, Segregated poly(vinylidene fluoride)/MWCNTs composites for high-performance electromagnetic interference shielding, Composites Part A 90 (2016) 606.
26. L.-C. Jia, D.-X. Yan, C.-H. Cui, X. Jiang, X. Ji, and Z.-M. Li, Electrically conductive and electromagnetic interference shielding of polyethylene composites with devisable carbon nanotube networks, J. Mater. Chem. C 3 (2015) 9369-9378.
27. R.K. Goyal, Cost-efficient high performance polyetheretherketone/expanded graphite nanocomposites with high conductivity for EMI shielding application, Mater. Chem. Phys. 142 (2013) 195-198.
28. C.-H. Cui, D.-X. Yan, H. Pang, X. Xu, L.-C. Jia, and Z.-M. Li, Formation of a segregated electrically conductive network structure in a low-melt-viscosity polymer for highly efficient electromagnetic interference shielding, ACS Sustainable Chem. Eng. 4 (2016) 4137-4145.
29. S. Maiti, S. Suin, N.K. Shrivastava, and B.B. Khatua, A strategy to achieve high electromagnetic interference shielding and ultra low percolation in multiwall carbon nanotube–polycarbonate composites through selective localization of carbon nanotubes, RSC Advances 4 (2014) 7979-7990.
30. L. Vovchenko, L. Matzui, V. Oliynyk, V. Launetz, Attenuation of electromagnetic radiation by graphite-epoxy composites, Phys. Status Solidi C 7 (2010) 12601263.
31. S. Pusz, U. Szeluga, B. Nagel, S. Czajkowska, H. Galina, and J. Strzezik, The influence of structural order of anthracite fillers on the curing behavior, morphology, and dynamic mechanical thermal properties of epoxy composites, Polym. Compos. 36 (2015) 336-347.
32. B. Kumanek, U. Szeluga, S. Pusz, A. Borowski, P. S. Wróbel, A. Bachmatiuk, J. Kubacki, M. Musioł, O. Maruzhenko, B. Trzebicka, Multi-layered graphenic structures as the effect of chemical modification of thermally treated anthracite. Fuller. Nanotub. Car. N. 26, (2018) 405-416.
33. B.D. Keller, N. Ferralis, and J.C. Grossman, Rethinking coal: thin films of solution processed natural carbon nanoparticles for electronic devices, Nano Lett. 16 (2016) 2951-2957.
34. S. Li S, X. Li, Q. Deng, and D. Li, Three kinds of charcoal powder reinforced ultra-high molecular weight polyethylene composites with excellent mechanical and electrical properties, Mater. Des. 85 (2015) 54-59.

35. L.L. Vovchenko, L. Y. Matzui, V.V. Oliynyk, and V.L. Launetz, The effect of filler morphology and distribution on electrical and shielding properties of graphite-epoxy composites, Mol. Cryst. Liq. Cryst. 535 (2011) 179-188.
36. L. Vovchenko, L. Matzui, V. Oliynyk, V. Launetz, V. Zagorodnii, O. Lazarenko, Electrical and Shielding Properties of Nanocarbon-Epoxy Composites, in: V. Mitchell (Eds.), Conductive Materials and Composites, Nova Science Publishers, New York, 2016, pp. 29-90.
37. J. Joo J, C.Y. Lee, High frequency electromagnetic interference shielding response of mixtures and multilayer films based on conducting polymers, J. Appl. Phys. 8 (2000) 513-518.
38. Z. Liu, G. Bai, Y. Huang, Y. Ma, F. Du, F. Li, T. Guo, and Y. Chen, Reflection and absorption contributions to the electromagnetic interference shielding of single-walled carbon nanotube/polyurethane composites, Carbon 45 (2007) 821-827.
39. D. Stauffer, A. Aharony, Introduction to percolation theory, Taylor and Francis, London, 1992.
40. M.O. Lisunova, Y.P. Mamunya, N.I. Lebovka, and A.V. Melezhyk, Percolation behavior of ultrahigh molecular weight polyethylene / multi-walled carbon nanotubes composites, Eur. Polym. J. 43 (2007) 949-958.
41. H. Gargama, S.K. Chaturvedi, A.K. Thakur, Design and optimization of multilayered electromagnetic shield using a real-coded genetic algorithm, Prog. Electromag. Res. B 39 (2012) 241-266.
42. Y. Danlee, I. Huynen, C. Bailly, Thin smart multilayer microwave absorber based on hybrid structure of polymer and carbon nanotubes, Appl. Phys. Lett. 100 (2012) 213105.
43. M. González, G. Mokry, M. Nicolás, J. Baselga, and J. Pozuelo, Carbon nanotube composites as electromagnetic shielding materials in GHz range, in: M.R. Berber, I.H. Hafez (Eds.), Carbon nanotubes-current progress of their polymer composites, InTech, 2016, ISBN 978-953-51-2470-2.
44. M.H. Al-Saleh, and U. Sundararaj, Electromagnetic interference shielding mechanisms of CNT/polymer composites, Carbon 47 (2009) 1738-1746.
45. H. Wang, D. Zhu, W. Zhou, and F. Luo, Effect of Multiwalled Carbon Nanotubes on the Electromagnetic Interference Shielding Properties of Polyimide/Carbonyl Iron Composites, Ind. Eng. Chem. Res. 54 (2015) 6589-6595.
46. D.M. Bigg, The effect of compounding on the conductive properties of EMI shielding compounds, Adv. in Polym. Techn. 4 (1984) 255-266.
47. P. Saini, V. Choudhary, B.P. Singh, R.B. Mathur, and S. Dhawan, Polyaniline–MWCNT nano-composites for microwave absorption and EMI shielding, Mat. Chem. Phys. 113 (2009) 919-26.
48. J.M. Thomassin, C. Jerome, T. Pardoen, C. Bailly, I. Huynen, C. Detrembleur. Polymer/carbon based composites as electromagnetic interference (EMI) shielding materials. Mater. Sci. Eng., R 74, 211–232 (2013)
49. M.H. Al-Saleh, U. Sundararaj, A review of vapor grown carbon nanofiber/polymer conductive composites, Carbon, 47 (2009) 2-22.
50. Y. Huang, N. Li, Y. Ma, F. Du, F. Li, X. He, X. Lin, H. Gao, and Y. Chen, The influence of single-walled carbon nanotube structure on the electromagnetic interference shielding efficiency of its epoxy composites, Carbon 45 (2007) 1614-1621.

51. N.C. Das, and S. Maiti, Electromagnetic interference shielding of carbon nanotube/ethylene vinyl acetate composites, J. Mater. Sci. 43 (2008) 1920-1925.
52. M. Arjmand, M. Mahmoodi, G.A. Gelves, S. Park, and U. Sundararaj, Electrical and electromagnetic interference shielding properties of flow-induced oriented carbon nanotubes in polycarbonate, Carbon 49 (2011) 3430-3440.
53. N.C. Das, Y. Liu, K. Yang, W. Peng, S. Maiti, and H. Wang, Single-walled carbon nanotube/poly(methyl methacrylate) composites for electromagnetic interference shielding, Polym. Eng. Sci. 49 (2009) 1627-1634.
54. A. Gupta, and V. Choudhary, Electromagnetic interference shielding behavior of poly (trimethylene terephthalate)/multi-walled carbon nanotube composites, Compos. Sci. Technol. 71 (2011) 1563-8.
55. C.-S. Zhang, Q.-Q. Ni, S.-Y. Fu, and K. Kurashiki, Electromagnetic interference shielding effect of nanocomposites with carbon nanotube and shape memory polymer, Compos. Sci. Technol. 67 (2007) 2973-2980.
56. Y. Xu, Y. Li, W. Hua, A. Zhang, and J. Bao, Light-Weight Silver Plating Foam and Carbon Nanotube Hybridized Epoxy Composite Foams with Exceptional Conductivity and Electromagnetic Shielding Property, ACS Appl. Mater. Interfaces 8 (2016) 24131-42.

**Figure Captions**

**Fig. 1.** SEM micrographs of the structures of graphene (a), TEG (b), and anthracite: raw (c) and after thermal treatment (d).

Fig. 2. The diagram of procedure of sample formation with segregated structure and the diagram of segregated systems with different amount of filler: below the percolation threshold, at the percolation threshold and above the percolation threshold (from left to right respectively).

**Fig. 3.** The evolution of conductive phase formation with increasing anthracite filler content in segregated composite A/PE: a – 1 vol.%, below $\varphi_c$; b – 3 vol.%, at $\varphi_c$; c – 5 vol.%, above $\varphi_c$.

**Fig. 4.** Concentration dependence of conductivity for composites with segregated structure and different carbon fillers. Inset shows the concentration dependence of conductivity for composites with anthracite filler for: (1) a segregated structure and (2) a random distribution of filler. Points are experimental values, lines correspond to the calculations from Eq. (2) for the region $\varphi > \varphi_c$.

**Fig. 5.** Shielding efficiency $SE_T$ (a) and reflection loss $RL$ (b) for PE-based composites with various filler content (number before type of filler means its volume content in vol.%) in the frequency range 26-37.5 GHz: 1 - 20Fe/PE, 2 - 10Cu/PE, 3 - 20Cu/PE, 4 - 2.5A/2.5Fe/PE, 5 - 2.5A/2.5Cu/PE, 6 - 10A/10Fe/PE, 7 - 10A/10Cu/PE. Thickness of samples $h$ =1.7 mm.

**Fig. 6.** Shielding efficiency $SE_T$ (a) and reflection loss $RL$ (b) for PE and PP based composites with various filler content in the frequency range 26-37.5 GHz: 1 - 1TEG/PE, 2 - 3.5TEG/PE,

3 - 5TEG/PE, 4 - 20A/PP, 5 - 20 A/PE, 6 - 2Gr/PE. Thickness of samples $h$ =1.0 mm.

**Fig. 7.** Schematic representation of multiple reflections in the segregated composite structure.

**Fig. 8.** Relationship between conductivity $\sigma$ and shielding effectiveness parameters of absorption $SE_A$, reflection $SE_R$ and total $SE_T$. Symbols are experimental values for different systems (corresponding to those given in Table 3), solid lines are calculations with Eqs (12) - (14) for carbon and hybrid fillers, and the dashed line is the calculation for the Cu/PE composite.

**Fig. 9.** a) the relationship between conductivity and shielding effectiveness SE according to the literature data and the results of this study; b) the effect of conductivity on reflection effectiveness $SE_R$. The symbols are experimental values; black solid lines are calculated by Eqs (12) - (14).

**Fig. 10.** Dependence of shielding effectiveness on the sample thickness. The line is guided by the eye.